energies

MDPI

Review

Analysis of Floating Offshore Wind Platform Hydrodynamics Using Underwater SPIV: A Review

Navid Belvasi [1,*], Frances Judge [1], Jimmy Murphy [1] and Cian Desmond [2]

[1] MaREI Centre, Environmental Research Institute, University College Cork, P43 C573 Cork, Ireland; frances.judge@ucc.ie (F.J.); jimmy.murphy@ucc.ie (J.M.)
[2] Gavin & Doherty Geosolutions Ltd., D14 X627 Dublin, Ireland; cdesmond@gdgeo.com
* Correspondence: nbelvasi@ucc.ie

Abstract: There is a need for new numerical tools to capture the physics of floating offshore wind turbines (FOWTs) more accurately to refine engineering designs and reduce costs. The conventional measurement apparatuses in tank tests, including wave probes, velocity and current profilers, and Doppler sensors, are unable to provide a full 3D picture of velocity, pressure, turbulence, and vorticity profile. In tank tests, use of the underwater stereoscopic particle image velocimetry (SPIV) method to fully characterise the 3D flow field around floating wind platforms can overcome some of the limitations associated with classical measurement techniques and provide a rich source of validation data to advance high-fidelity numerical tools. The underwater SPIV method has been widely used for marine and offshore applications, including ship and propeller wakes, wave dynamics, and tidal stream turbines; however, to date, this technology has not seen widespread use for the hydrodynamic study of FOWTs. This paper provides a critical review of the suitability of underwater SPIV for analysing the hydrodynamics of FOWTs, reviews the challenges of using the method for FOWT tank test applications, and discusses the contributions the method can make to mitigating current research gaps in FOWT tank tests.

Keywords: floating offshore wind turbine; FOWT; high-fidelity; numerical tools; stereoscopic particle image velocimetry; SPIV; advanced tank test methods; model test

Citation: Belvasi, N.; Judge, F.; Murphy, J.; Desmond, C. Analysis of Floating Offshore Wind Platform Hydrodynamics Using Underwater SPIV: A Review. *Energies* **2022**, *15*, 4641. https://doi.org/10.3390/en15134641

Academic Editor: Antonio Rosato

Received: 1 June 2022
Accepted: 22 June 2022
Published: 24 June 2022

1. Introduction

Considering the 30 MW Hywind Scotland wind farm, the 24 MW WindFloat project in Portugal, and upcoming projects including the 30 MW EFGL in France and the 88 MW Hywind Tampen developments [1], Europe is on course to become a world leader in floating offshore wind. Current estimations for floating offshore wind turbines (FOWTs) suggest that the cost of energy will fall by 70% and reach 40 EUR/MWh by 2050, while total installed capacity is expected to increase to 250 GW [2]. However, these cost reductions are not guaranteed and will require robust design tools to enable designers to balance cost reduction, structural integrity, and project risk. A wide variety of engineering design tools with a limited representation of the underlying physics have been developed and employed for FOWT hydrodynamical design [3]. These numerical codes have been based on either frequency or time-domain analysis. A comprehensive review of the current state of the art of numerical tools in the field of FOWTs was carried out in [4].

As low-fidelity models, frequency-domain codes utilise a combination of potential flow theory and the Morison equation, or each separately. Potential flow theory uses strip theory, the panel method, or a combination of both. This method has limitations, as discussed in [4]. These limitations include ignoring the viscous effect, along with considering a small wave oscillation amplitude compared with the cross-section area of the floater. Moreover, the interaction of the flow and the structure between the floater members is not addressed accurately. While this approach reduces the computational requirements, its limited capacity to capture the low-frequency motion of the floating platform results in inconsistencies and errors. These errors can be up to a 20% difference in the mean value of the results [5]. The Morison equation, on the other hand, considers a term for viscous effects along with inertia effects, hence it can used to evaluate the force on a submerged thin body in an oscillatory flow [6]. This semiempirical method has also some limitations, such as considering a uniform flow acceleration at the location of the body, validity for only very large or very small Keulegan–Carpenter numbers [7], and providing a poor representation when applying nonunidirectional flow, such as for a horizontal cylinder in a spread sea.

Accurately capturing turbulence modelling is essential for response analysis of floaters so that engineers can produce reliable and cost-effective designs in terms of motion response, fatigue load estimation, and the structural and mooring design of FOWTs. Compared with frequency-domain codes, time-domain codes, including full computational fluid dynamics (CFD) simulations, provide a more complete picture of platform responses as nonlinearity is considered. CFD codes provide high-fidelity data such as turbulent kinetic energy, velocity distribution, mean velocity, vorticity profile, flow wakes, fluid flow interaction with floater members, and the wave-making characteristics of the floater [8]. These high-fidelity numerical approaches have a significant computational expense compared with linearised engineering models; however, their use is necessary to resolve detailed flow phenomena and the system response. The accuracy in the CFD simulation results can be limited by numerical errors, an inseparable part of digital computation. A study on the accuracy of turbulence models was undertaken in [9], which revealed that the uncertainty levels for a demonstration of a model's wake in fluid flow could reach 30% near the wall of the model. There is a requirement for validation data to reduce inaccuracies and errors in these high-fidelity numerical simulations.

In both frequency- and time-domain numerical approaches, there is a lack of accurate verification data. As FOWT technologies advance, high-fidelity models will see greater adoption, and so the validation of these advanced models will be critical. Tank testing and real-world demonstrations are sources of validation data, though higher-accuracy measurement apparatuses are required to fully resolve flows and response. In tank tests, the single-point wave measurement equipment includes wave probes, laser Doppler velocimeters (LDV), and acoustic Doppler velocimeters (ADV). Additionally, for current measurements, there are velocity profilers such as acoustic Doppler current profilers (ADCP) and pitot tubes. These are practical tools that measure fluid velocity at individual points in the tank. These measurements apparatus are subject to their associated errors; a comprehensive review of underwater speedometer equipment and its measurements errors was provided in [10]. Using only these instruments, it is impossible to fully and accurately understand the tank flow regime with regard to, for instance, full velocity and pressure distribution contours, Reynolds stresses, specific dissipation rate (SDR), turbulent kinetic energy (TKE), and TKE production and dissipation rate (TDR) behind the model in tank. Therefore, a complete 3D picture of the fluid flow cannot be produced for the validation of high-fidelity numerical models.

Comprehensive flow characterisation can be achieved by stereoscopic particle image velocimetry (SPIV). SPIV is an optical measurement technique in which the velocity field of an entire interrogation area within the flow is measured simultaneously. This is the fundamental advantage of SPIV over single-point measurement methods. Other characteristics of turbulent flow, as mentioned in the previous paragraph, can then be derived from the velocity field. SPIV facilitates both the extraction of measurement data and the visualisation of flow structures. An optical nonintrusive technique, it allows a complete picture of the turbulent flow field to be produced and reveals insights about the study domain, for instance, velocity, turbulent kinetic energy, and vorticity distribution. Moreover, as a high-fidelity method, the resolution of data captured by SPIV is equivalent to several thousand measuring points in an assumed interrogation window (See Figure 1). Therefore, in an assumed spatial volume, the fluid flow parameters can be measured with high resolution. The SPIV technique is widely used for studying the aerodynamics of offshore wind turbines (Figure 2) (e.g., [11–13]) and for the validation of complementary CFD simulations [14]. Additionally, some researchers have used the SPIV technique to study other marine renewable technologies [15]; however, the use of underwater SPIV for FOWT tank tests is an emerging field. There has been only one published research paper on the topic to date [16], investigating the scale effect of heave plates in a floating wind turbine with a semisubmersible floater with underwater PIV measurements. The SPIV method can be used to fully characterise the 3D flow field around floating platforms in the laboratory environment, provide a rich source of validation data, and overcome some of the limitations associated with conventional equipment for measuring fluid flow [17].

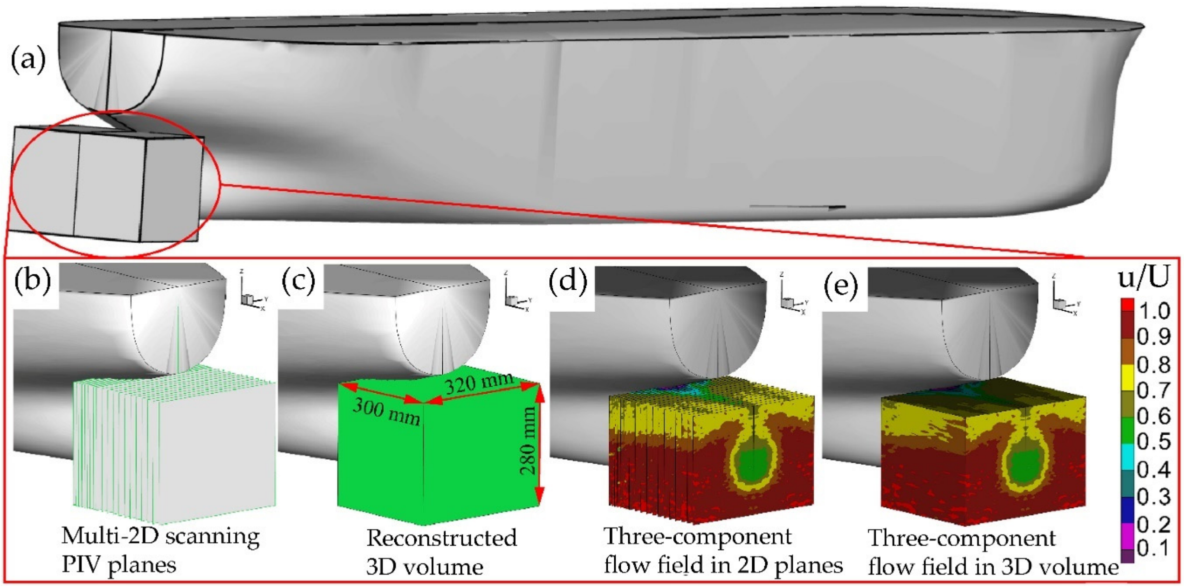

Figure 1. Reconstruction procedure of 3D-3C flow with multiple 2D-3C SPIV velocity planes [18]: (**a**) area of interest at the model aft; (**b**) locations of multiple-2D scanning SPIV planes; (**c**) reconstructed 3D volume; (**d**) three-component flow field in 2D planes; (**e**) three-component flow field in 3D volume.

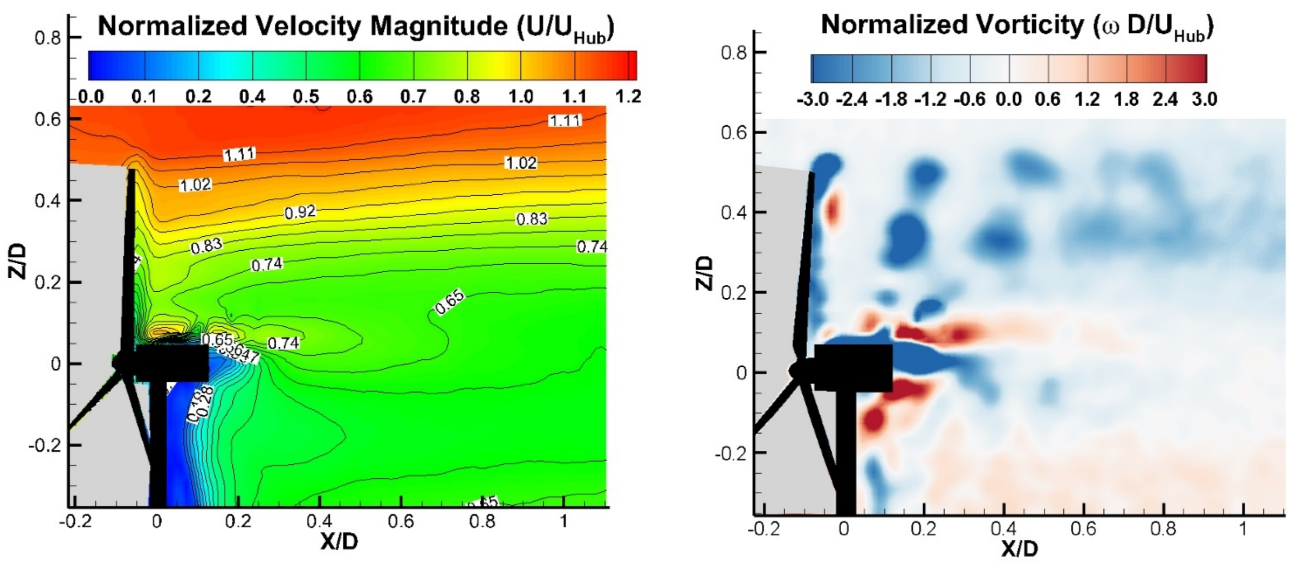

(**a**) (**b**)

Figure 2. Stereoscopic PIV measurements of a wind turbine wake [19]: (**a**) Normalized velocity magnitude (TKE); (**b**) Normalized vorticity.

Fluid flow around the FOWT substructure is three-dimensional and unsteady; it is a turbulent flow with a transient and rotational nature, such that a separation region could also form around the elements of the body in this nonuniform flow. It is incompressible, and viscous effects can be dominant depending on the incident wave and the shape of the platform. In Table 1, the geometric features of four floater types for FOWT applications are presented. The hydrodynamics of the SPAR platform, which are due to its simple, circular shape, could act as an inertia- or viscous-dominant body in different incident wave conditions. If the Keulegan–Carpenter (KC) number for the platform is less than 3, the platform has an inertia-dominant nature due to incoming waves, while for $3 < KC < 15$, it can be assumed that the floater drag, in wave force loading terms, has a linear nature. Moreover, for $15 < KC < 45$, the shape of the drag force follows a nonlinear trend, such that low-fidelity models such as the Morison equation cannot accurately anticipate the applying wave force [20]. The hydrodynamics of barge-type floaters are easier to study because of their simple shape. However, there is some inconsistency when studying the effect of moonpool size on the platform hydrodynamics in wave conditions with a period near the resonance period of the floater [21]. Concerning other platform types, i.e., semisubmersibles and TLPs, there can be complicated interactions between different elements of the body, such as the bracelet and main columns and the fluid flow. Low-fidelity models are unable to provide a compressive dynamic fluid body interaction (DFBI) analysis to provide a clear picture of this fluid flow interaction or of the wake area. High-fidelity models such as CFD can provide this full picture, and the validation data produced by PIV can significantly improve these numerical models as well as providing a benchmark that could aid researchers when selecting the mesh quality, a suitable equation for the wall condition based on the platform condition (e.g., to model marine growth on the floater), a turbulence model, and an appropriate value for tuning the turbulence model equations based on the flow regime and wave conditions. Since both CFD and SPIV can provide visualisation and numerical results that can be compared with each other, SPIV could act as a validation reference for CFD measurements.

Table 1. General description of the geometry of main categories of FOWT substructures (references for projects and images: row 1, [22]; row 2, [23]; row 3, [24]; row 4, [25]).

Floater Type	Example Project	Particulars [m]		Schematic
Semisubmersible	DeepCwind	Draft Freeboard Mid-column diameter Outer-column diameter Column spacing Cross braces diameter	20 10 6.5 12 50 1.6	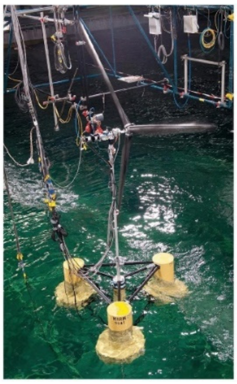
SPAR buoy	OC3-SPAR	Draft Freeboard Column diameter above taper Column diameter below taper Taper height	10 120 6.5 9.4 8	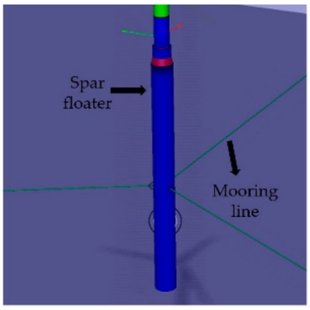

Table 1. *Cont.*

Floater Type	Example Project	Particulars [m]		Schematic
Barge platform (with rectangular moonpool)	NEDO	Draft Freeboard Length Breadth Skirt offset	7.5 2.5 48 48 3	
Tension leg platform (TLP)	GICON TLP	Draft Waterline to tower bottom Length Breadth	30.7 37.25 32 32	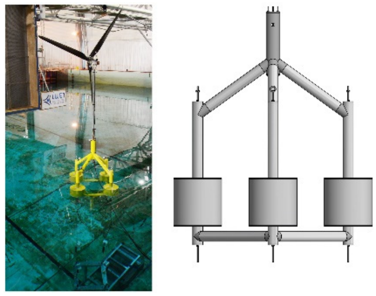

Comprehensive reviews on particle image velocimetry measurements have been widely published in the literature. For example, the review conducted by Abdulwahab et al. [26] provided a compressive investigation on the evolution of particle image velocimetry, its operational principals, and uncertainty and errors. In another review study conducted by Westerweel et al. [27], the state of the art and the applicability of the method for measuring complex and turbulent flows were reviewed, and the past development in PIV measurement in order to reduce the method uncertainty was discussed. A summary of different implementations of the PIV method, such as PIV itself, SPIV, and tomographic PIV, along with their limitations and challenges in the field, was provided by Kähler et al. [28].

The current review paper aimed to provide its readers with the state of the art of underwater SPIV measurements in tank testing and identify opportunities for using the method in FOWT tank test campaigns to better understand the flows around the floater and provide a rich source of validation data for advanced numerical models. Despite the high-resolution results of SPIV, there are uncertainties associated with the laser frequency, tracer particle response, and hardware synchronisation in addition to limitations on the studied platform scale, data sampling rate, and SPIV instrumental setup for FOWT hydrodynamical measurements. Therefore, key considerations for SPIV use in FOWT tank tests are discussed in this paper. This review paper covers the vast majority of these parameters in the following sections, to act as a guideline to mitigate these barriers.

The remainder of this paper is divided into four main sections. In section two, the state of the art of PIV in tank tests is reviewed. Ship hydrodynamics, waves, and flow around simple primary geometric shapes such as cylinders in wave tanks are discussed. Because of different setup requirements for FOWT tank testing, there are challenges to making measurements in practice; these are presented and discussed at the end of Section 2. Section 3 discusses the application of this method for FOWT hydrodynamic analysis as well as providing guidelines for its use in FOWT tank testing. Conclusions are provided in Section 4.

2. Underwater SPIV Measurements for FOWT Tank Tests

In this section, the main applications of SPIV in tank tests are reviewed. In should be noted that in terms of the dynamics of the platform and the SPIV apparatus setup, using SPIV for ship applications is different from using it for FOWT applications. Whereas in ship applications, the PIV device is attached to the towing carriage in a towing tank, for FOWT applications, the platform is usually moored in a fixed location. Having a stationary SPIV system for FOWT tank testing measurements could cause several challenges, which are discussed in Section 2.2. Although the behaviour may be different, there are similarities in the hydrodynamics measured, such as the wake area, vortices around the body, and the drag. Additionally, the shape of current FOWTs is generally a combination of simple geometric shapes such as cylinders, box sections, etc. Therefore, careful attention must be given to the application of SPIV for measuring fluid flow interactions with these shapes. Moreover, it is important to review the application of SPIV for wave analysis, since it drives the loading applied on floaters.

2.1. State of the Art of Particle Image Velocimetry in Tank Tests

The basis of PIV is the measurement of the displacement of particles in fluid at different time steps. The fluid flow is filled with traceable particles, and a laser passed through a lens generates a flat light sheet that illuminates the particles. The PIV measurement is achieved by group tracking of fluid particles and processing their trajectory at different time intervals. By high-frame imaging of the illuminated particles and postprocessing of consecutive images, the particle groups' displacement is extracted for each time step, and their relative velocities are calculated using a group distance and a sample time (See Figure 3). This travelling distance depends on parameters such as flow rate, camera frame rate, and the level of fluid flow turbulence. Since this method is an indirect measurement, the movement of tracer particles within the fluid flow is examined instead of the flow attributes being determined. Therefore, the type and properties of particle seeds are chosen based on the studied fluid and turbulence.

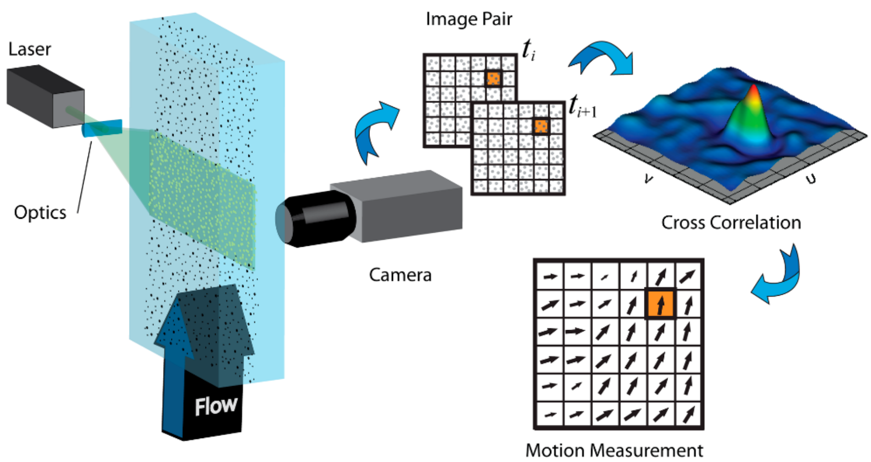

Figure 3. Schematic description of the PIV principle [29].

Various methods, such as Gaussian, phase discrimination, and dynamic mean value operator, have been developed to review and postprocess PIV raw data [30]. These image comparison methods can later be distinguished from each other in their local or global regularisation schemes. Global schemes iteratively optimise the entire flow field and its displacement path, while in local methods, a number of interrogation windows are selected, and the group paths of particles inside these windows are investigated in consecutive images. This iterative phase is repeated for all captured images in the interrogation windows. A well-known approach to conducting this iterative step is the cross-correlation method. A review of the theory of the cross-correlation method and its application in particle image velocimetry was conducted in [31], where the fundamentals of this method were comprehensively discussed.

PIV was first used for tank testing in [32]. The main motivation of this research was to investigate wave structure near the bow of a ship model. The test was performed using a camera and an underwater light sheet. After processing the data, the researchers extracted a two-dimensional velocity field for a 3.05 m ship model in flow with a Froude number in the range of 0.17 to 0.45. These measurements also determined the velocity near the free surface. In this study, special focus was placed on flow vorticity production and its energy losses. This result was significant, as the PIV method visualised the turbulence intensity and the 3D velocity distribution in the tank test campaign (see Figure 4).

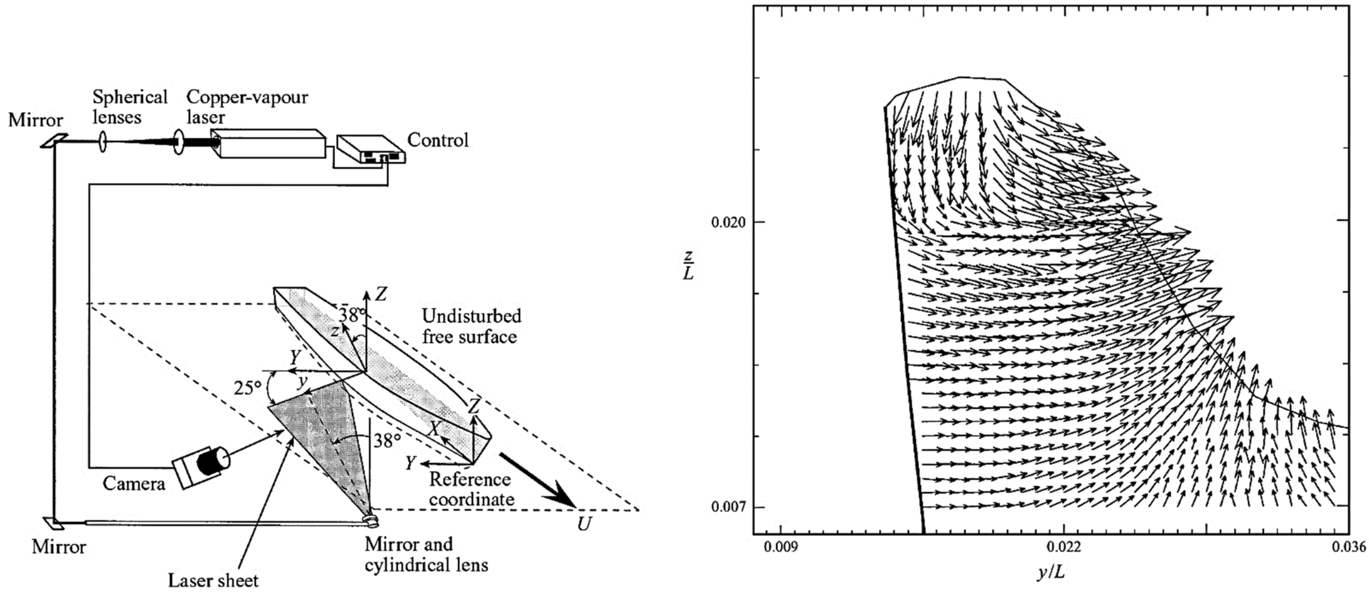

(**a**) (**b**)

Figure 4. Dong's PIV Experiments [32]: (**a**) PIV setup; (**b**) magnitude portion of the velocity field.

Tukker et al. [33] studied the feasibility of using the PIV technique to measure the unsteady spatial structure of flow in test tanks. Attention was paid to the main features of PIV in test tanks, including the seeding of a large quantity of water and the visibility of the particles in water, as well as measuring the accuracy of the method. For the first time, a digital camera was used for PIV in a test tank. A 64×64 pixel interrogation window was used to record the wake area behind a passing ship model. The PIV equipment was stationary, which limited the study to examining only one area of the ship path. However, the study was beneficial, since it could visualise the unsteady and spatial flow dynamics around a model. Ref. [33] showed that using a higher-resolution digital camera increased the frame accuracy and quality of data for the two-dimensional plane. Using this method in a tank test was promising, since it could record the instantaneous flow velocity measurements. However, the use of 2D PIV caused out-of-plane velocity error, which is calculation error for the velocity vectors in the third dimension normal to the light sheet.

In the research described above, all PIV experiments recorded only two-dimensional velocity vectors, and the error in the third dimension was due to the particles leaving the thin light sheet. This error in the third dimension is known as the ubiquity problem. This is a disadvantage, since the flow structure after the model has a significant 3D characteristic. In the single-camera method, the particle velocity can be calculated correctly only in two dimensions on the laser screen. In the SPIV method, the particle velocity in the third dimension can also be obtained by postprocessing of vectors [34]. Therefore, by recording the images on two cameras, the actual velocity vector in the third dimension can be calculated with a geometric reconstruction (see Figure 5).

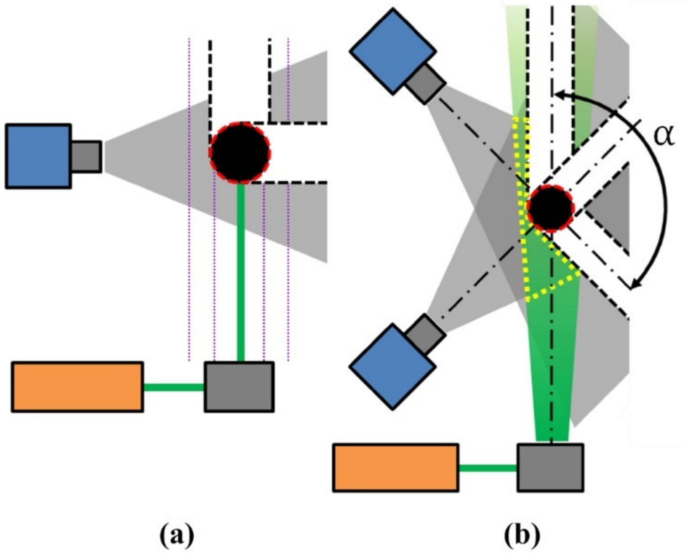

Figure 5. Comparing PIV and SPIV techniques to solve the ubiquity problem for the out-of-plane vectors [35]: (**a**) schematic of PIV setup; (**b**) schematic of S-PIV setup.

An important parameter in SPIV tests is the angle of the cameras relative to the light sheet. Lee et al. conducted a sensitivity analysis [36] and extracted the maximum value of the error related to in-plane and out-of-plane velocity vectors for different camera angles (see Figure 6). The research showed that the ideal camera angles were symmetrical at 45 degrees to the light sheet, which may not be suitable for all test campaigns, depending on the dimensions of the model, the dimensions of the basin, and the distance of the cameras to the illuminated plane.

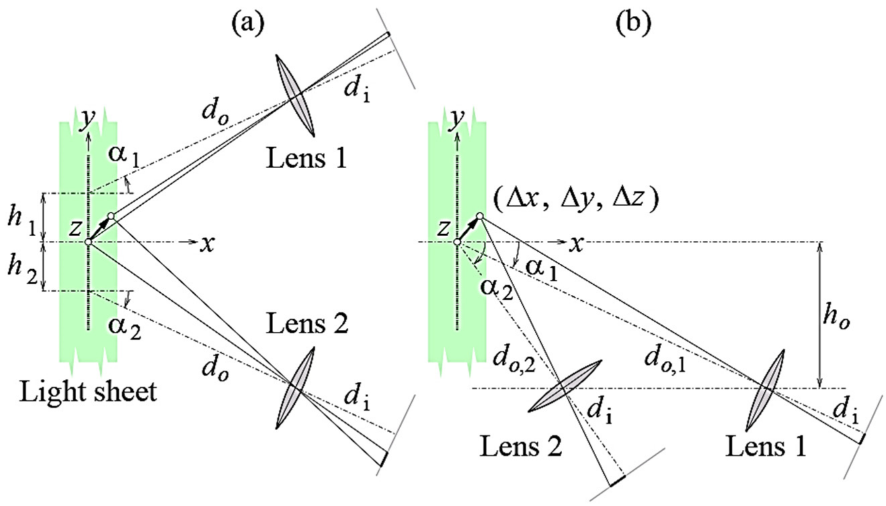

Figure 6. Camera arrangement in SPIV tests [36]: (**a**) symmetric or asymmetric rotational (SR); (**b**) rotational translational (RT) at a fixed distance.

Research was conducted on various types of SPIV systems with different arrangements consisting of two vertical cylinders [37]. The purpose of the experiment was to study the generated vortex of a 3.047 m ship model. The new design allowed for the capture of vortices with a frequency of 3 Hz. The distributions of velocity and vorticity were used to characterise vortices. Since the PIV method can capture and visualise the instantaneous velocity and vorticity fields, the vortices in the fluid flow could be captured simultaneously. Having an accurate estimation of vortices around the model can improve the design to reduce undesired phenomena such as vortex-induced vibration and motion (VIV and VIM, respectively), multibody flow interaction, wave–current–body interaction, sloshing, and the instantaneous position of wave load. Additionally, this estimation can lead to a better understanding of flow wake around the floater model, which can in turn lead to an accurate estimation of floater motion in different environmental conditions.

SPIV equipment is widely used in marine and offshore engineering applications and has contributed significantly to the study of wave kinematics, especially phenomena such as wave breaking. For example, ref. [38] was a study of the small-scale turbulence under the wind wave surface boundary layer, its dissipation rate and vertical profile, and the surface shear velocities. The study concluded that measurements of small-scale turbulence with conventional instruments such as acoustic Doppler velocimeters (ADV) were difficult because of the pointwise data provided by these devices. However, the SPIV measurements enabled the researchers to review small-scale turbulence properties on the order of 10^{-6} to 10^{-3}, such as vorticity and dissipation rate. These characteristics were directly measured by calculating the instantaneous spatial velocity gradients form the 3D velocity vectors provided by SPIV.

The effect of wave breaking over a sloping beach was examined experimentally using PIV in [39]. In this study, the full space–time evolution of the velocity field was measured for several test cases, and the void fraction between the air and water phases in each point of the domain is examined. The research helped to obtain the terms of the fluctuating kinetic energy transport equation [40] for a 1:5 sloped beach.

Since the FOWTs usually have hull shapes consisting of basic geometric elements, it is important to review the applicability of underwater SPIV in tank testing these types of elements. An example is [41], which focused on flow field measurements around a surface-piercing cylinder with free surface effects. This research investigated free surface effects on the development of a turbulent boundary layer around the cylinder. Within the Froude number range of 0.126 to 0.40, as well as the equivalent Reynolds number range of 395,000 to 1,250,000, the free-surface effect, development of retarded wake, and wave-induced separation around the model were visualised and measured.

In another study [42], the fluid flow behind intersecting and tapered cylinders was investigated with the use of underwater SPIV. In this study, with a sampling rate of 15 Hz, the vortex shedding dislocations presented in the vortex sheet behind the cylinder were captured, and their relationship with the Reynolds number was investigated. The range of Strouhal numbers was 0.19 to 0.26. As concluded in this study, performing underwater SPIV tank testing has inherent complexity in regard to controlling the seeding density and apparatus calibration technique, since the device is submerged.

SPIV is a suitable tool for studying turbulence flows in tank tests; however, it is critical to limit the uncertainty of the method in test campaigns. Yoon et al. carried out a benchmarking investigation by examining a ship model with a length of 3.048 m using the SPIV system. The first aim of the research was to create a manoeuvre database for that model [43]. The second aim was to develop a systematic method for examining the SPIV uncertainties, setting the validity criteria on converging error, and performing a standard uncertainty assessment. The test campaign was carried out for pure yaw and sway tests. Moreover, the results included the axial velocity and turbulent kinetic energy at the measurement sections (See Figure 7). The convergence error of the test campaign was less than 1% of the towed velocity Uc for the velocity distribution field. Additionally, the standard uncertainty was in the range of 2–3% of Uc for the velocity fields.

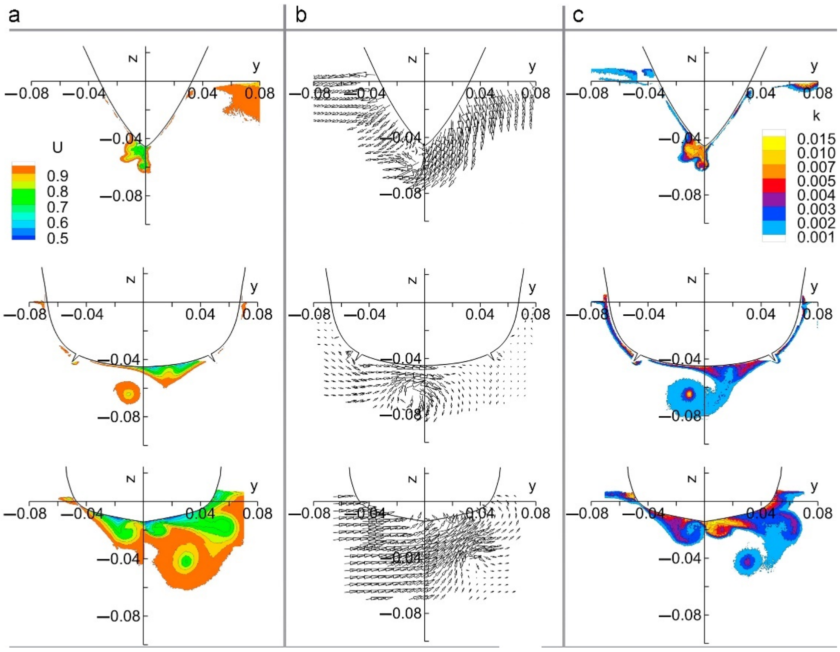

Figure 7. PIV results of pure yaw tests: (**a**) axial velocity; (**b**) cross-plan VW vectors; (**c**) turbulent kinetic energy [43].

In the underwater SPIV technique, the equipment, including the cameras and laser, is kept underwater. These attachments may influence the flow regime by causing backflow and interaction with the flow around the model. This issue was examined by Han et al., who investigated the uncertainties of the SPIV method for its application in tank testing [44]. A ship model with a Froude scale of 1/100 in both uniform flow and nominal wake flow was studied. Two digital cameras were used to undertake a detailed examination. In order to quantitatively assess the high-fidelity results, the procedure proposed by ITTC [45] and the method proposed by Yoon [43] were utilised. In their experiment, with having a 14 Hz sampling rate, it was found that the torpedo configuration of the SPIV system did not significantly affect the computational velocity field and the resulting error was negligible. The nominal wake-field measured in that study is shown in Figure 8. The study showed that data obtained with the SPIV technique were both accurate and high resolution. Moreover, the equipment in this technique did not interfere with the fluid flow.

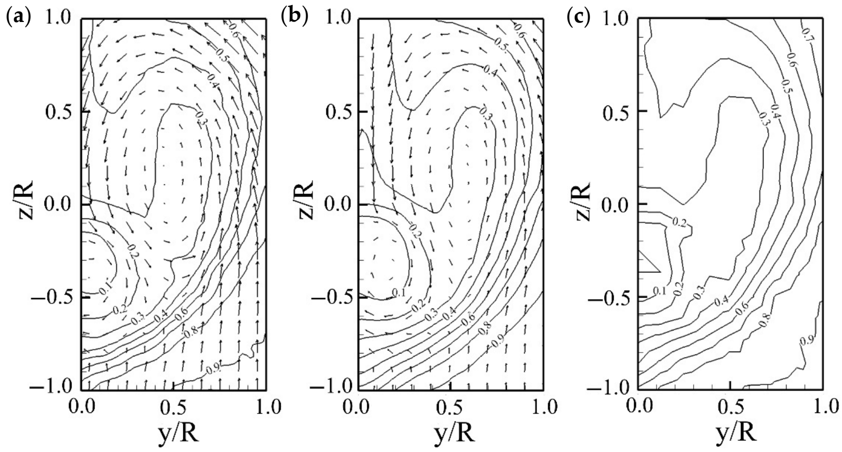

Figure 8. Nominal wake-fields for a model in different measuring techniques (contour lines are $\overline{u}$, and the vectors are tangential velocity components) [44]: (**a**) SPIV result; (**b**) PIV result; (**c**) Pitot-static tube result.

To date, the use of underwater SPIV in tank tests has been limited to the study of ship propellers [46], tidal stream turbines [47], ship model wave fields [33,48], and general phenomena such as vortex-induced vibrations [49]. There have been successful attempts in the literature to use this technology to create a high-fidelity ship manoeuvring database [43]. The same approach can be used for the hydrodynamic study of FOWTs with regard to minimising the uncertainty of velocity measurements in the test campaign. High-resolution data on vorticity, full velocity distribution, and turbulent kinetic energy then can be used as a source of validation data for numerical codes for FOWTs. In [50], the applicability of a tunned LES turbulence model for studying the flow around an equilateral triangular cylinder was analysed. Having the SPIV data enabled the study to reach less than 5% error between LES and PIV methods for parameters such as the streamwise velocity and Reynolds stress correlation.

To date, there has been only one published study [16] applying underwater PIV for the investigation of the hydrodynamics of FOWTs. The study aimed to investigate the scale effect on the kinematics of an oscillating heave plate using underwater PIV measurements with a sampling rate of 15 Hz. One column of HiPRWind FOWT [51] was modelled in three different Froude scales of 1:20, 1:27.6, and 1:45.45. A complete set of velocity and vorticity fields was extracted, which showed significant similarities in the results among different scales used. All of the produced vortex shedding had similar shapes, velocity contours, and centre positions. The study showed that the scale effect was negligible in the experimental study of heave plates, helping other researchers to choose desirable scales for their heave plate studies based on their laboratories' limitations.

Although SPIV could be beneficial for studying FOWT hydrodynamics, there are a variety of associated challenges to using the method for FOWT tank tests. In the next subsection, these are discussed.

2.2. Challenges of Underwater SPIV Measurements for FOWT Tank Tests

The associated issues for underwater PIV measurements in tank tests include seeding of the tank with traceable particles, the out-of-plane velocity of particles, illumination in water, imaging techniques, and different camera angles and the associated uncertainties. These issues accompany the scale limitations of the platform and instrumental setup for FOWT tank testing, limitations in reaching a suitable sampling frequency, the effect of the apparatus setup on the platform's hydrodynamics, and laboratory policies on safety hazards regarding laser use. These challenges are discussed in this section.

2.2.1. Particle Seeds

The SPIV technique is an indirect approach, so instead of the flow being directly examined, the response of illuminated particles in the flow is analysed. Therefore, in particle selection, the particle mass and the optical reflectance are important. In seeding selection, other factors, such as the distribution of particles and the seeding density in the fluid, should also be studied for each test; these criteria were well studied in [30]. The primary sources of error are the effects of gravity and buoyancy on the motion and response of particles. Particles with lower density than the fluid follow the fluid path very well (see Figure 9). However, the cumulative effect of collisions between particles and the fluid vortex causes unwanted random movement of the particles. This random motion is called Brownian motion [52], leading to measurement errors up to 15% of fluid flow velocity [53]. Contrarily, coarse particles with density higher than that of the fluid do not respond well to fluid flow turbulence [54].

The reflectivity of the particles is another topic of interest. Coated glass particles are commonly used in underwater PIV testing. Their uniform dimensions and excellent reflectivity attributes make them suitable for underwater application. However, in typical wave basins [55], the need for high quantities of particles for several tests makes coated glass an uneconomical option. Fluorescent particles can also be used, as they avoid unwanted reflection of the model surface and bubbles. However, these particles are expensive. Suitable alternatives are Orgasol and Vestosint particles [56], which have the same reflectance qualities and good economic efficiency. Ashworth Briggs et al. recently proposed a practical alternative to these conventional particles during their test campaigns [49]. In that study, a series of fluorescent particles with 57 mm mean diameter were fabricated and coloured with Rhodamine 6G. The uncertainty of the experiment was reduced to 0.5 mm. Nonetheless, choosing the right particles should be based on test conditions and the phenomenon under study, with focus on issues such as seeding a tank with dimensions [57] of 35 m length, 12 m width, and 3 m depth. The wave basin tank is a nonclosed loop system, so conducting FOWT SPIV measurement would require continuous seeding for the test section where the FOWT platform is moored.

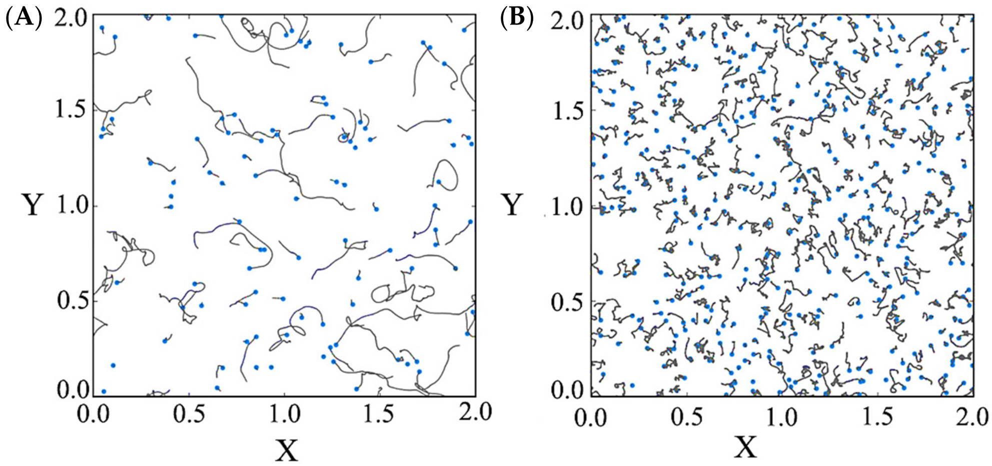

Figure 9. Trajectories of vortices [58]: (**A**) coarse seeding, $Ek = 1 \times 10^{-4}$; (**B**) dense seeding, $Ek = 7 \times 10^{-6}$.

2.2.2. Illumination

Lasers are among the integral components of PIV measurements. These elements create monochromic light with high energy density. Passing this light through an optic lens turns it into a thin light sheet (See Figure 10), which illuminates the particles in PIV measurements. In comparison with aerodynamics, in hydrodynamics, the fluid is denser, and it is necessary to use higher-power lasers for illumination. Among early PIV experiments, a 20 MJ laser was used in the tank test described in [32]; more recently, ND YAG lasers provided illumination power of up to 200 MJ at a wavelength of 532 nm [26]. At this maximum energy, the maximum practical repetition frequency was within the range of 7–25 Hz. The laser frequency must be synchronised with the camera shooting frequency, and the repetition rate of the laser radiation should be adjusted according to the imaging rate. For example, a laser with a power of 200 MJ has an approximate repetition frequency of 20 Hz; if a higher frequency is needed, the laser power should be decreased. However, this results in less illumination in the water medium and lower image quality. In terms of FOWT measurements, this issue could overlap with the safety requirements for lab testing, since specific requirements need to be met for laser operation. Having a class-4 laser in order to provide suitable illumination for the measurements could bring extra lab safety requirements to the test campaign [59] in terms of laser hazards and laser operation. Additionally, guiding the laser beam to the area of the investigation is also important, since some areas of investigation could be within the platform elements in order to investigate their interactions in fluid flow.

Another issue is the high reflection from the model surface in the water environment (see Figure 10), which is due to the high laser illumination. Reflection problems at or near the model wall boundary due to high laser illumination can lead to errors and have been examined in various studies. Sciacchitano investigated the reduction of errors in this area as well as the overall reduction of method uncertainty [60]. A comprehensive methodology for studying this error and introducing approaches to prevent it in a PIV campaign was given in [61]. A possible solution to this issue is to paint the model black or fabricate the model using acrylic material. However, it is not possible to make complex models, such as those that would be required for FOWT testing, out of these materials.

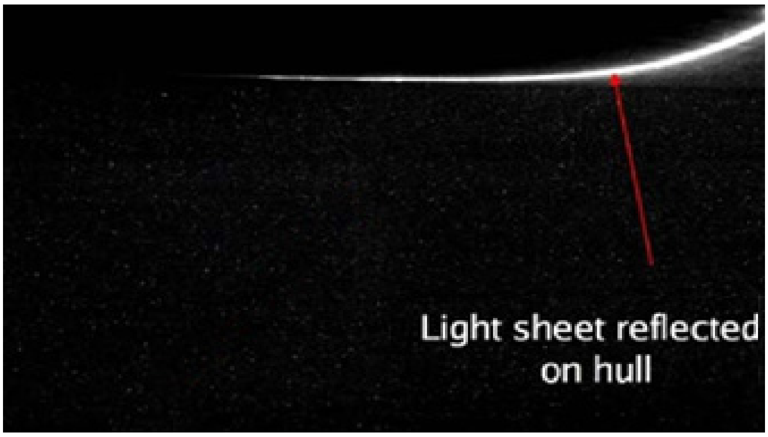

Figure 10. Reflection issue due to high illumination [62].

In the PIV method, the velocity components are usually calculated on a two-dimensional light sheet. Using only one camera results in a perspective error, as any out-of-plane movement of particles leads to an error in calculating the third-dimension vectors [63]. This error is reduced using the SPIV method (two cameras), although the accuracy of the results may still be affected, since the technique is based on 2D assumptions, and any particle motion vector outside the particle plane affects the results.

Several particles that move across the illuminated light sheet could affect the light sheet's intensity in different images. The particles disappear when leaving the light sheet, and the new particles are replaced constantly; this affects the postprocessing schemes' error [64]. This random error is one of the fundamental and dominant errors in the SPIV method. A recommended approach to mitigating this error is to ensure that less than a quarter of the particles leave the light sheet between each two laser pulses [61]. In order to limit out-of-plane loss, ref. [30] proposed several methods for recording particle paths; however, each of these methods has its own advantages and disadvantages. One approach is to divide the time interval between pulses. The velocity is obtained by reconstructing the movements in a time interval [58]. Therefore, this method reduces the fluctuations of the constructed velocity field both in the third dimension and on the light sheet plane.

2.2.3. CCD Cameras and Image Processing

The advantage of the SPIV over the PIV method is using two digital cameras instead of one; thus, the third velocity vector is calculated correctly with a geometric reconstruction of images, and the associated error is reduced. However, the presence of two cameras with different angles leads to a loss of a part of the interrogation window. Moreover, the lenses' angles and the requirement for a mapping technique result in a relative error in the overall calculation of the velocity field. Various arrangements for the two cameras were suggested in [30]. However, a 45-degree angle is an optimal angle in terms of error reduction to an error ratio of 1 percent [36]. Jurgens et al. also investigated this issue in their study [65] and proposed a symmetrical setup for two cameras to reduce the error. Although this type of arrangement usually has the least error for the third velocity vector, it strongly affects the vector and fluid distribution around the model. In any case, the dimensions of the model, the tank test, and the interrogation window are the three primary parameters that set the distance and angle of the cameras to the light sheet.

After capturing the raw image data, there are a significant number of outliers, and the raw data need to be preprocessed. Image processing in the SPIV method usually has three main phases [66]: (1) data validation and velocity vectors (outliners) extraction, (2) a replacement scheme, and (3) data assimilation. A comprehensive review of many of these preprocessing algorithms' advantages and disadvantages was carried out in [27]. Many researchers have worked on optimising these algorithms [67]; however, one of the most valid methods for this purpose is the global histogram filter [68].

Researchers have worked on developing different schemes to investigate the uncertainty of SPIV and the parameters that have the greatest impact on uncertainty. Among the well-known and widely used methods are the uncertainty surface method [69], multipulse and multiframe methods [27], the peak ratio method [70], and particle disparity [60]. These schemes and their governing mathematical equations were thoroughly discussed and reviewed in [30,60,61,64]. The study area in tank testing usually has a significant three-dimensionally turbulent characteristic. Many parameters, such as image pixel size, particle strength and density, velocity gradients, turbulence variation, and noise level [71], are involved in error generation and raise the uncertainty of this method. In the previous two decades, researchers have tried to identify and reduce these error sources [30,60,70,72–74]. One well-known method for this is the uncertainty surface [69], in which captured images are analysed for parameters affecting the error. However, the scale of the FOWT platform and the trade-off between the quality of the image and the area of the investigation in each test case is an issue discussed in the next subsection.

2.2.4. Scale Issues in Model Testing

The particle image velocimetry measurement is limited by the field of view, i.e., the investigation area, in each test run. While reaching greater fields of view (for example, up to 400 mm $\times$ 400 mm in [75]) is possible by adjusting the cameras, the need for high-power lasers (more than 200 mJ) to illuminate this area properly constitutes a limit to reaching larger investigation areas in practice. In the most recent underwater PIV measurement, the field of view was approximately 250 mm $\times$ 300 mm [16].

The model scale ratio is typically chosen in the range of 1:30–100 for FOWT tank testing [76]. Larger scale ratios (less than 30) are limited by the tank basin size, as well as economic considerations, whereas smaller scale ratios cause an increase in uncertainty, a decrease in repeatability, and a larger scale effect in extrapolating the results to full-scale size [77].

Given the size of the FOWT prototype in, for instance, the OC4 project [78] (see Figure 11), a tank testing scale ratio of 1:50 results in a model with a height of 600 mm and a spacing of 1 m between offset columns (see Table 2). This model size makes SPIV an inconvenient solution for conducting a 3D full measurement for the whole platform in a reasonable time schedule, since in each test case, SPIV measurements can be conducted for one wave/current condition in a 2D area of a maximum of 30 mm $\times$ 300 mm. To have a full 3D picture, for only one test case (one wave/current condition), several measurements at different planes with small offsets in between would need to be conducted. Moreover, in some areas in the vicinity of the model, for example, between the main and offset columns, it is difficult to conduct measurements, since other components shadow the image of the middle components; moreover, the cameras and laser gun cannot be placed in the middle of the platform because of practical limitations on arrangement to date. Changing the SPIV arrangement for a regulator test condition out of the shadowing area would require a new setup and thus reinstallation and recalibration of the apparatus. Considering this matter along with processing time leads to an extended tank test time, which brings extra costs to the measurement campaign.

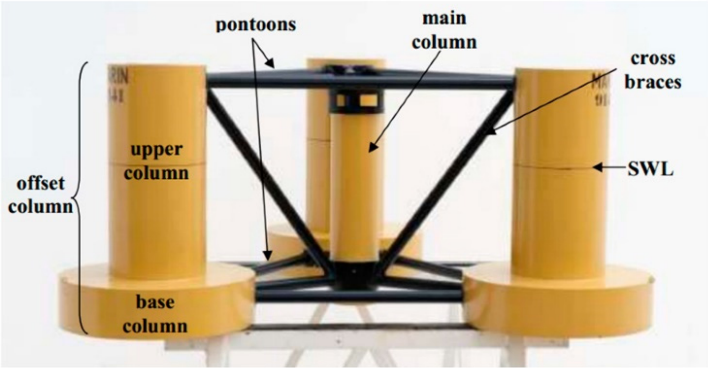

Figure 11. Schematic of a semisubmersible floater of the OC4 project in model scale [79].

Table 2. OC4 platform dimensions in prototype and scaled sizes.

Particulars	Prototype (m)	Scaled Model 1:50 (mm)
Total draft (SWL)	20	400
Tower base elevation (above SWL)	10	200
Offset columns elevation (above SWL)	12	240
Offset columns spacing	50	1
Tower base dimeter	6.5	130
Offset columns dimeter (base)	24	480
Offset columns dimeter (upper part)	12	240
Length of offset columns (base)	6	120
Length of offset columns (upper part)	26	520
Diameter of pontoons and cross braces	1.6	32

2.2.5. Instrument Setup and FOWT Degrees of Freedom

Although the FOWT tank test could have some minor similarly to ship model tank testing, in regard to wake measurements, degree of freedom, etc., the SPIV setup would be significantly different in some cases. While in ship tank testing, the PIV setup can be attached to the carriage and move along the model in the test section (see, for example, [80]), in FOWT tank testing, the platform is moored in an area of the tank, and the movement of the platform is investigated. If a fixed SPIV apparatus were used in FOWT tank testing, the platform would have movement inside and outside of the illumination area, causing an inconsistency in the data that would require the application of further postprocessing algorithms and thus lead to a more time-consuming process.

The SPIV method is limited by the blockage of the optical path, so offset elements could block the laser beam, causing a shadow on the elements behind them. Although the platform shape is much simpler in term of curvature than the shape of ship models, having bracelets in the model and connections between different elements of the platform would cause limitations to installing the SPIV setup in any location around or inside the floater, so that a vast majority of the area could not be measured with SPIV because of possible clashing due to the platform's movement.

2.2.6. Sampling Frequency

The SPIV setup cannot be considered a time-resolved method, since capturing some phenomena requires acquiring a much higher sampling frequency than the current practical limit of 15 Hz [48]. Having a 15 Hz sampling rate results in a 7.5 Hz Nyquist frequency [81] in frequency-domain analysis, so only phenomena with a frequency lower than this limit can be comprehensively studied. As an example, it is difficult to derive the added mass value from SPIV results, since it is related to acceleration measurements. At the moment, it is difficult to obtain acceleration from SPIV, since this would require acquiring a higher sampling frequency than 15 Hz [16]. Therefore, any phenomena with a transient nature might not be captured with these high-fidelity measurement methods because of practical limits to reaching to a proper sampling rate. Therefore, with the current development of SPIV, only the time-averaged field of the flow characteristics and the steady-state phase of the FOWT hydrodynamics are guaranteed.

2.2.7. Effect of the SPIV Apparatus's Presence in FOWT Tank Testing

The presence of the SPIV device could have an effect on the hydrodynamic behaviour of the platform, since having these two in the vicinity of each other could cause interaction on the platform dynamics. Although some SPIV setups, such as the torpedo (see [48]), could have a lower effect on the platform because of their hydrodynamical shape, in practice, it is not possible to have them in the vicinity of the floater. Thus, PIV investigation is limited to the far wake area of the platform or at a sufficient clearance. The effect of body interaction in wave conditions has been widely discussed in the literature for different body shapes, both numerically and experimentally (for example, see [82,83]). Therefore, while conducting SPIV measurements in FOWT tank test, having interaction between the studied FOWT model and the SPIV apparatus is inevitable. This requires further investigation and analysis of the effects on the fluid flow disturbance and induced drag terms of each SPIV setup used.

3. Application of Underwater SPIV to Mitigate Current Research Gaps in FOWTs Tank Tests

A variety of hydrodynamical phenomena can be studied with underwater SPIV. The main contributions of this technique are in the fields of wave kinematics, viscosity study, and the characteristics of the turbulence in the flow around the floaters. Hydrodynamical phenomena related to floater design and their degrees of importance are outlined in Table 3, which is based on studies in the OC5 project [84,85].

Table 3. Hydrodynamical phenomenon identification ranking developed based on the OC5 project (H: high, M: medium, L: low).

Row	Phenomena	Importance	Physics Understanding	Validation Needs	Suitability of Underwater SPIV for Providing Validation Data
1	VIV/VIM substructure	M	L	H	Yes
2	Nonlinear excitation—diff/sum/mean	H	M	H	Yes
3	Short-crested waves	M	H	H	Yes
4	Marine growth influence on loads	L	H	L	Yes
5	Breaking/steep wave loads	L	M	H	Yes
6	Wave–current–body interaction	H	M	M	Yes
7	Viscous load model	H	M	H	Yes
8	Multibody flow interaction	H	M	H	Yes

3.1. Vortex-Induced Vibration and Motion

One field in which SPIV contributes to FOWT design is the study the vorticity field behind the model. This could be beneficial for studying problems such as vortex-induced vibration and motion. An experiment on the flow-induced oscillations of a floating model SPAR-type floater was conducted in [86]. The model was a 1:470 scale model of the Hywind SPAR platform. In this study, the amplitude and frequency of the platform response were captured by tracker cameras. Moreover, wake visualisation was carried out by snapshooting smoke behind the model. In this experiment, in the frequency analysis, the spectrum range captured was within the range of 0 to 4 Hz for both cross-flow and inline-flow motions of the platform. Using SPIV in this type of study could be beneficial, since the vorticity core in the Z direction (normal to the water surface) can be captured and visualised, and this can be done in different shedding frequencies in the range lower than the in-practice Nyquist frequency limit of 7.5 Hz for the SPIV method. Research to date has used cameras to find only the trajectory of the floater motions. Using SPIV could be beneficial, since it could help to visualise the vortex in experimental tests. Then, the trajectory of these vortices and their excitation region can be identified. This valuable data can then be used to minimise the VIV effect and analyse different VIV suppression methods, for instance, by reviewing different strake shapes on the model.

3.2. Nonlinear Wave Loads

SPIV results could be used to study nonlinear wave effects on the floater, as the linear wave assumption has considerable error for wave loading and platform response estimation. Among the ongoing research, in [87], the effect of nonlinear assumptions on motion analysis of a FOWT with a semisubmersible floater was reviewed. It was shown that compared with nonlinear wave assumption, linear wave theory led to overestimations of 17.6% for pitch and 24.6% for heave responses of the platform. Having an optical method for extracting the velocity and turbulence field could provide more data to develop a scheme to mitigate this difference between wave theories.

A study on the effects of fully nonlinear wave loads on FOWTs was conducted in [88]. In this study, the effects of linear and fully nonlinear wave loads on an OC4 semisubmersible platform were examined. The focus of this study was mainly on floater motion, structural responses, and mooring line tension due to nonlinear and linear waves. The parameters taken into account were the wave free-surface location and velocity distribution near the platform. Other results that were studied included the wave spectra at different frequency ranges. The SPIV method could make a great contribution here, since it is an instantaneous and visual method. Having an experimental visualisation of the velocity field for incident and diffracted waves around the floater could help to better understand the relation of the different incident waves with the loading centre on the platform, as well as the characteristics of vortex stretching behind the platform in each wave regime.

3.3. Short-Crested Waves

The substructure of a FOWT is a large-scale bluff body, so the presence of the substructure in the incident waves makes scattered waves in the vicinity. As a classical approach, diffraction theory can be used to study the hydrodynamics of these bluff bodies in waves. As discussed in [89], although diffraction theory is a practical approach to modelling wind-generated waves, these waves are modelled more realistically with short-crested waves. The application of short-crested waves has been a matter of interest for many researchers to date [90–92].

A variety of studies on short-crested waves have been conducted in the literature, one of which was an experimental study on the directional hydrodynamic coefficient and wave force due to the spreading angles of these waves [93]. In this study, the wave surface elevation and force exerted on a cylinder model were studied. A range from 0 to 45 degrees was considered for directional spreading angles. Then, the relation of this parameter with the Keulegan–Carpenter (KC) number was reviewed. The main results of this study were the wave time history, wave elevation, and wave force on the model with regard to the spreading angles. From the optical perspective, SPIV could have an indirect contribution to the study of short-crested waves. Although this method cannot be used for direct measurements of applied forces, changes in the wave elevation can be extracted in real time. SPIV can be useful for bringing 3D velocity vectors to form time- and depth-averaged velocity contours. Having the velocity field in this elevation studied could help to identify the vertical vorticity profile and its variation or to formulate a relation between the 3D turbulence structure of short-crested waves and their heights and angles of incidence to the floater.

3.4. Marine Growth's Influence on Loads

There are strong ways for SPIV to contribute to the study of marine growth's effect on FOWTs. Marine growth could have different effects on the substructure of FOWTs. Marine growth increases the thickness, structural weight, drag coefficient, and hydrodynamical added mass of the platform. The effect of marine growth on the dynamics of offshore wind support structures has been studied by many researchers. In [94], for example, special focus was given to the effects of the zonation and thickness of marine growth on the mode shape and natural and bucking frequencies of the supporting platform. In order to estimate the wave force, the drag and inertia coefficient were calculated based only on offshore standards and guidelines [95,96]. The main variation in the drag and inertia coefficients due to marine growth was related to the thickness and distribution of the growth, the Keulegan–Carpenter number, the relative surface tension, and the direction of incident waves. The drag component's integration could be conducted with the SPIV method. This drag interrogation could be aligned with the inflow, with the crossflow, and in specific directions, for instance, with vortex drags. These results could be used to study marine growth's effect on the floater drag coefficient with different feasible growth thickness and distributions. Since the results is based on quantitative optic measurement, SPIV could also be used to study the turbulence and vortex generation of marine growth on the floater, which could help to develop a new roughness function model that represents marine growth for wall boundaries used in numerical analysis, for example, unsteady RANS simulations in CFD.

SPIV experiments could also be used to study the effect of marine growth on tendon and mooring line responses. Marine growth has an influence on the mooring lines and umbilical cables. This could happen by increasing their diameter. Although in practice this thickness increase is considered as an ideal and homogeneous roughness, studies have shown that this idealisation is not valid for realistic conditions in the sea. In realistic situations, a great portion of marine growth could be attached to specific portions of mooring lines. A study on the effect of marine growth on FOWT mooring lines was carried out in [97], in which the dynamic behaviour of mooring lines under the effect of different quantities and distributions of marine growth was studied. In this study, different distributions of marine growth were considered, and for each test case, the tensions and effective tension in anchor and fairlead points were investigated. In [98], conventional equipment such as load cells was mainly used to study the responses of an FOWT's mooring line. However, SPIV could also have a contribution to this topic. Different materials can be used for FOWTs' mooring lines, such as synthetic ropes, chains, and wire ropes. Marine growth could have a different effect on each of these materials, such as different intensities or distributions of growth on them. SPIV could be utilised along with loadcells so that while the tension in both the fairlead and anchor points is provided, the hydrodynamic behaviour of mooring with marine growth can be examined in interrogation windows along the mooring length. Moreover, in the case of using the tendon, the pattern of vortex shedding of the mooring could be investigated; this pattern could then be formulated to find a relation among different mooring configurations, the VIV of the mooring line, and the platform's responses.

3.5. Breaking/Steep Wave Loads

An important field that SPIV can play a role in is the quantitative estimation of the breaking/steep wave loading on FOWTs. When breaking waves occur, a mixture of air and water create a turbulent flow region. This air–sea interface has a complex structure. Laboratory research on breaking waves in deep water was conducted in [99], which was mainly focused on wave-breaking rates and wave-following turbulent dissipation. There has also been some effort in the literature to simulate this phenomenon's effect on fixed and moored floating with the SPH (smoothed particle hydrodynamics) method [100]. However, as these studies have reviewed, the magnitude of this phenomena has been overestimated by up to 30% in numerical cases. SPIV could be beneficial here, since it could help to extract instantaneous velocity components and vectors for each sequence of breaking wave. Then, other related parameters of turbulence, such as time-dependent turbulent kinetic energy, Reynolds stress, and turbulence production and dissipation, could be extracted. These data could then be used to distinguish between different wave-breaking cases (where the velocity around the floater could be considered two-dimensional with neglectable variation in the z direction, or vice versa) Moreover, the share of wave energy transferred to the turbulent kinetic energy (TKE) can be examined. Additionally, the data can be used to find a relation between accumulated vortices in the wake area of the floater and the secondary load cycle applied to the floater due to wave-breaking phenomena.

3.6. Wave–Current–Body Interaction

The interaction of gravity waves and surface mean flow could have a complex structure, which means that SPIV could be utilised to investigate this phenomenon. Current could act as a damping source for long structures [101]. Moreover, the current makes frequency and shape modifications to the wave; hence, the interaction of the incident current and waves with the structure could be a matter of interest in FOWT motion analysis. Research was carried on wave–current interaction's effect on a 5 MW FOWT with an OC3-Hywind SPAR floater [102]. In this study, the FOWT's response under waves with and without current interaction was studied. The results were mainly tower displacement, floater displacement, and mooring tensions at fairleads. In this study, it was shown that the simple method of superposing the wave and current effects caused overestimation of the response of the FOWT. This difference caused an overestimation of 12% in the mooring tension force. SPIV could be used for the study of wave kinematics with and without current interaction; the SPIV velocity and verticity results on this complex turbulent structure could be used for different wave and current propagation angles. Moreover, the floater's wave making in load cases can be reviewed quantitatively.

3.7. Viscous Load Model

Viscous loads are an important load case in FOWT analysis, since the viscosity could have different effect on the floater. Among the different phenomena caused by viscosity, the viscous drift forces in extreme sea states [21] and the viscous damping (also known as eddy-making damping) effect [103] on the floater and mooring line are worth mentioning. FOWT models with second-order potential-flow theory usually underestimate forces and results compared with CFD and lab-testing approaches [104]. This is mainly due to ignoring the separation and viscous drag in potential-flow theory.

As was proven in [105], the viscosity field for a pseudoplastic flow could be captured with SPIV method. In this study, both momentum conservation equations and rheological models were replaced with SPIV data. Therefore, the viscosity field was examined indirectly. Moreover, it was shown that well-known approaches in determining viscosity effects, such as the power law and the Carreau–Yasuda model, resulted in unrealistic increases in viscosity estimation. This kind of research could be reestablished for studying FOWTs and Newtonian fluids. Notably, the wake structure and the shares of pressure, viscosity, and kinetic energy in this structure could be visualised and examined. These data would be beneficial for enhancing the estimation and formulation of viscosity's share in numerical models while analysing the wave and current loading applied on the floater.

3.8. Multibody Flow Interaction

SPIV results could also have a contribution in developing other novel approaches in FOWT analysis, for instance, multibody modelling. Much research has been carried out on utilising the multibody method for FOWT analysis, for example, [106–108]. Some of this research focused mainly on coupling this method with numerical methods such as potential theory and CFD [107]. SPIV could have an important, though indirect, contribution in this field. Since the multibody approach is usually coupled with numerical models, such as the CFD and BEM methods, SPIV data could act as a replacement or validation source for hydrodynamic data provided by CFD. Research on the uncertainty of the CFD method for analysis of FOWTs was conducted in [109]. In this study, the total uncertainty of CFD for estimating the difference-frequency heave force was on the order of 51%. Using underwater SPIV data instead of CFD for coupling with the multibody method could mitigate the relevant errors and uncertainties, which could be an interesting topic for further investigation.

4. Discussion and Conclusions

This paper provides a review of the applicability of SPIV in FOWT tank tests, since there is a need for high-fidelity data to aid the development of emerging numerical tools and for validation of the new CFD and SPH codes to develop FOWTs. FOWT tank tests currently tend to rely on the use wave probes, Doppler sensors, pitot tubes, and current profilers. Additionally, the use of these instruments results in more manipulation of the fluid flow and measurement error. As an alternative, fluid flow measurement can be conducted with underwater SPIV. The SPIV method is an underutilised technique in FOWT design and has the capacity to provide critical validation data for high-fidelity numerical tools. Since the technology is seeing emerging application in FOWT hydrodynamic tank test, it is beneficial to have a review on the method, issues critical for its new application, and a discussion on its contributions to filling the research gaps in FOWT tank testing.

A review of the challenges of underwater SPIV use for FOWT tank testing is provided. It is discussed that with the use of SPIV, the unsteady structure of turbulent flow around the floater can be measured and understood. However, because of the need for using different setups for SPIV apparatuses and different approaches for tank testing a FOWT platform moored in a certain location of the tank, using a stationary SPIV apparatus could bring complexity to the FOWT SPIV measurements. A summary of these limitations is provided in Table 4.

Table 4. Challenges of underwater SPIV use for FOWT tank testing.

Row	Challenges	Importance	Already Addressed in Literature on the Underwater SPIV Method
1	Particle seeds	Seeding of a large-volume tank	Yes
2	Illumination	Illumination in water	Yes
3	CCD cameras	Error associated with imaging and postprocessing	Yes
4	Scale issues	Trade-off between platform scale and area of investigation for SPIV, since large scale is preferable for FOWT tank testing, while the area of investigation is limited in SPIV	No
5	SPIV apparatus and platform movement	The apparatus is fixed in place, while the platform is moored in a certain section of the tank and has degrees of freedom	No
6	Sampling rate of SPIV	Having a 15 Hz sampling rate in practice, limited underwater SPIV to be used for investigating phenomena with a steady-state nature or to review a platform with a time-averaged perspective	No
7	Effect of apparatus on hydrodynamical behaviours of the floater	The presence of the SPIV apparatus could influence the floater behaviour; study must be conducted on this interaction	No

The paper also provides a review of the phenomena and research gaps related to FOWT tank testing. It was concluded that the SPIV method could mitigate the current limits in reviewing these phenomena and advance the state of the art in FOWT tank testing. These phenomena and topics include VIV, nonlinear wave loads, short-crested wave loading, marine growth's effect on floater hydrodynamics, breaking/step wave loads, wave–current–

body interactions, vicious load models, and multibody interactions. The contributions of underwater SPIV to each of these research topics are summarised in Table 5.

Table 5. Contributions of underwater SPIV to current research gaps in FOWT hydrodynamics.

Row	Phenomenon/Research Topic	Current Physics Understanding	Contributions of Underwater SPIV
1	VIV/VIM of substructure	L	▪ Visualising the vortex in experimental test ▪ Studying the trajectory of vortices and their excitation region ▪ Analysing different VIV suppression methods,
2	Nonlinear excitation—diff/sum/mean	M	▪ Extracting full 2D/3D velocity field for incident and diffracted wave around the floater in experimental test ▪ Studying the wave-loading centre on the platform, as well as the characteristics of vortex stretching behind
3	Short-crested waves	H	▪ Accurate wave elevation and surface level change due to short-crested wave ▪ Three-dimensional velocity vectors to form time averaged and depth averaged velocity contours. ▪ Identifying vertical vorticity profile and its variation ▪ Providing high-fidelity contours to formulate a relation between the 3D turbulence structure of short crest-waves and their heights and angles of incidence to the floater
4	Marine growth's influence on loads	H	▪ Analysing the turbulence and vortex generation of marine growth on the floater (reviewing different thickness and distribution of growth) ▪ Integrating drag terms (analysing the contribution of marine growth to local turbulence generation and its share in overall drag forces) ▪ Deriving velocity and turbulence data from SPIV investigation of marine growth would be beneficial for developing a new roughness function model that represents marine growth for wall boundaries used in numerical analysis
5	Breaking/steep wave loads	M	▪ Extracting instantaneous velocity components and vectors for sequences of breaking waves ▪ Extraction of time-dependent turbulent kinetic energy, Reynolds stress, and turbulence production and dissipation in the wave-breaking process ▪ Using data to distinguish between different wave-breaking cases, where the velocity around the floater could be consider two-dimensional with neglectable variation in the z direction, or vice versa ▪ Examining the share of wave energy transferred to the turbulent kinetic energy (TKE) for different breaking cases ▪ Deriving a relation between accumulated vortices in the wake area of the floater and the secondary load cycle applied to the floater during wave breaking
6	Wave–current–body interaction	M	▪ Studying wave kinematics with/without current interaction ▪ Using the SPIV velocity and verticity results on a complex, turbulent structure for different wave and current propagation angles ▪ Quantitatively reviewing the floater's wave making in wave–current loading cases and comparing it with that in wave-only cases

Table 5. *Cont.*

Row	Phenomenon/Research Topic	Current Physics Understanding	Contributions of Underwater SPIV
7	Viscous load model	M	▪ Examining the viscosity field around the floater ▪ Studying the floater's hydrodynamic wake structure and the shares of pressure, viscosity, and kinetic energy in this structure ▪ Using data to enhance the estimation and formulation of viscosity's share in drag force estimation with numerical models for FOWT application
8	Multibody flow interaction	M	▪ Potentially acting as a replacement or validation source for hydrodynamic data provided by CFD/BEM in multibody approaches ▪ Reducing the CFD method's uncertainty by providing validation data in terms of the turbulence budget of the flow around the floater

Underwater SPIV as a validated tool will contribute to our understanding of hydrodynamical phenomena such as those identified by the OC5 project as contributing to uncertainty in the design of floating offshore wind turbines. With established best-practice guidelines, SPIV can make a significant contribution to reducing the uncertainty, and ultimately the cost, of FOWT. The current paper will bridge the gap between the SPIV method and floating wind research communities in terms of both physical and numerical analysis and encourage greater collaboration focused on the high-potential research areas identified in Section 3. We hope that this paper will serve to raise awareness of the opportunities and challenges associated with the use of SPIV in this rapidly developing field.

Author Contributions: N.B. conceptualised the research, conducted the literature survey and review, wrote the paper, and reviewed and edited the paper; C.D. conceptualised the research, acquired the funding, provided supervision, and reviewed and edited the paper; F.J. reviewed and edited the paper; J.M. provided supervision, supervised the research team, and reviewed and edited the paper. All authors have read and agreed to the published version of the manuscript.

Funding: This research is performed in the framework of the FLOAWER project. This project received funding from the European Union's Horizon 2020 research and innovation programme under the Marie Skłodowska-Curie grant agreement N° 860879.

Institutional Review Board Statement: Not applicable.

Informed Consent Statement: Not applicable.

Data Availability Statement: Not applicable.

Conflicts of Interest: The authors declare no conflict of interest.

References

1. Wind Europe. *Floating Offshore Wind Is Gearing up for Take-Off*; Wind Europe: Brussels, Belgium, 2020.
2. DNV GL. *Floating Wind: The Power to Commercialize*; DNV GL: Bærum, Norway, 2020.
3. Cordle, A.; Jonkman, J. State of the Art in Floating Wind Turbine Design Tools. In Proceedings of the Twenty-First International Offshore and Polar Engineering Conference, Maui, HI, USA, 19–24 June 2011.
4. Otter, A.; Pakrashi, V.; Robertson, A.; Murphy, J.; Desmond, C. Review of Modelling Techniques for Floating Offshore Wind Turbines. *Wind Energy* **2021**, *1*, 831–857. [CrossRef]
5. Rahimi, H.; Dose, B.; Stoevesandt, B.; Peinke, J. Investigation of the Validity of BEM for Simulation of Wind Turbines in Complex Load Cases and Comparison with Experiment and CFD. *J. Phys. Conf. Ser.* **2016**, *749*, 012015. [CrossRef]
6. Morison, J.R.; Johnson, J.W.; Schaaf, S.A. The Force Exerted by Surface Waves on Piles. *J. Pet. Technol.* **1950**, *2*, 149–154. [CrossRef]
7. Ren, C.; Lu, L.; Cheng, L.; Chen, T. Hydrodynamic Damping of an Oscillating Cylinder at Small Keulegan–Carpenter Numbers. *J. Fluid Mech.* **2021**, 913. [CrossRef]
8. Liu, Y.; Xiao, Q.; Incecik, A.; Peyrard, C.; Wan, D. Establishing a Fully Coupled CFD Analysis Tool for Floating Offshore Wind Turbines. Renew. *Energy* **2017**, *112*, 280–301. [CrossRef]

9. Rezaeiha, A.; Montazeri, H.; Blocken, B. On the Accuracy of Turbulence Models for CFD Simulations of Vertical Axis Wind Turbines. *Energy* **2019**, *180*, 838–857. [CrossRef]
10. Fuentes-Pérez, J.F.; Meurer, C.; Tuhtan, J.A.; Kruusmaa, M. Differential Pressure Sensors for Underwater Speedometry in Variable Velocity and Acceleration Conditions. *IEEE J. Ocean. Eng.* **2018**, *43*, 418–426. [CrossRef]
11. Bayati, I.; Bernini, L.; Zanotti, A.; Belloli, M.; Zasso, A. Experimental Investigation of the Unsteady Aerodynamics of FOWT through PIV and Hot-Wire Wake Measurements. *J. Phys. Conf. Ser.* **2018**, *1037*, 052024. [CrossRef]
12. Xiao, J.P.; Wu, J.; Chen, L.; Shi, Z.Y. Particle Image Velocimetry (PIV) Measurements of Tip Vortex Wake Structure of Wind Turbine. *Appl. Math. Mech.* **2011**, *32*, 729–738. [CrossRef]
13. Wang, Z.; Ozbay, A.; Tian, W.; Sharma, A.; Hu, H. An Experimental Investigation on the Wake Characteristics behind a Novel Twin-Rotor Wind Turbine. In Proceedings of the 33rd Wind Energy Symposium, Kissimmee, FL, USA, 5 January 2015.
14. Desmond, C.J.; Watson, S.J.; Aubrun, S.; Ávila, S.; Hancock, P.; Sayer, A. A Study on the Inclusion of Forest Canopy Morphology Data in Numerical Simulations for the Purpose of Wind Resource Assessment. *J. Wind Eng. Ind. Aerodyn.* **2014**, *126*, 24–37. [CrossRef]
15. Day, A.H.; Babarit, A.; Fontaine, A.; He, Y.P.; Kraskowski, M.; Murai, M.; Penesis, I.; Salvatore, F.; Shin, H.K. Hydrodynamic Modelling of Marine Renewable Energy Devices: A State of the Art Review. *Ocean Eng.* **2015**, *108*, 46–69. [CrossRef]
16. Anglada-Revenga, E.; Bezunartea-Barrio, A.; Maron-Loureiro, A.; Molinelli-Fernandez, E.; Oria-Escudero, J.; Saavedra-Ynocente, L.; Soriano-Gomez, C.; Duque-Campayo, D.; Gomez-Goni, J.; Souto-Iglesias, A. Scale Effects in Heave Plates: PIV Investigation. In Proceedings of the International Conference on Offshore Mechanics and Arctic Engineering, Online, 3–7 August 2020.
17. Chen, P.; Chen, J.; Hu, Z. Review of Experimental-Numerical Methodologies and Challenges for Floating Offshore Wind Turbines. *J. Mar. Sci. Appl.* **2020**, *19*, 339–361. [CrossRef]
18. Wu, T.; Deng, R.; Luo, W.; Sun, P.; Dai, S.; Li, Y. 3D-3C Wake Field Measurement, Reconstruction and Spatial Distribution of a Panamax Bulk Using Towed Underwater 2D-3C SPIV. *Appl. Ocean Res.* **2020**, *105*, 102437. [CrossRef]
19. Premaratne, P.; Tian, W.; Hu, H. A Proper-Orthogonal-Decomposition (POD) Study of the Wake Characteristics behind a Wind Turbine Model. *Energies* **2022**, *15*, 3596. [CrossRef]
20. Konstantinidis, E.; Bouris, D. Drag and Inertia Coefficients for a Circular Cylinder in Steady plus Low-Amplitude Oscillatory Flows. *Appl. Ocean Res.* **2017**, *65*, 219–228. [CrossRef]
21. Tan, L.; Ikoma, T.; Aida, Y.; Masuda, K. Mean Wave Drift Forces on a Barge-Type Floating Wind Turbine Platform with Moonpools. *J. Mar. Sci. Eng.* **2021**, *9*, 709. [CrossRef]
22. Tran, T.T.; Kim, D.-H. A CFD Study of Coupled Aerodynamic-Hydrodynamic Loads on a Semisubmersible Floating Offshore Wind Turbine. *Wind Energy* **2018**, *21*, 70–85. [CrossRef]
23. Putri, R.M.; Obhrai, C.; Jakobsen, J.B.; Ong, M.C. Numerical Analysis of the Effect of Offshore Turbulent Wind Inflow on the Response of a Spar Wind Turbine. *Energies* **2020**, *13*, 2506. [CrossRef]
24. Kosasih, K.M.; Suzuki, H.; Niizato, H.; Okubo, S. Demonstration Experiment and Numerical Simulation Analysis of Full-Scale Barge-Type Floating Offshore Wind Turbine. *J. Mar. Sci. Eng.* **2020**, *8*, 880. [CrossRef]
25. Walia, D.; Schünemann, P.; Hartmann, H.; Adam, F.; Großmann, J. Numerical and Physical Modeling of a Tension-Leg Platform for Offshore Wind Turbines. *Energies* **2021**, *14*, 3554. [CrossRef]
26. Abdulwahab, M.; Ali, Y.; Habeeb, F.; Borhana, A.; Abdelrhman, A.; Al-Obaidi, S. A Review in Particle Image Velocimetry Techniques (Developments and Applications). *J. Adv. Res. Fluid Mech. Therm. Sci.* **2020**, *65*, 213–229.
27. Westerweel, J.; Elsinga, G.E.; Adrian, R.J. Particle image velocimetry for complex and turbulent flows. *Annu. Rev. Fluid Mech.* **2013**, *45*, 409–436. [CrossRef]
28. Kähler, C.J.; Astarita, T.; Vlachos, P.P.; Sakakibara, J.; Hain, R.; Discetti, S.; La Foy, R.; Cierpka, C. Main Results of the 4th International PIV Challenge. *Exp. Fluids* **2016**, *57*, 97. [CrossRef]
29. Ismadi, M.-Z.; Higgins, S.; Samarage, C.R.; Paganin, D.; Hourigan, K.; Fouras, A. Optimisation of a Stirred Bioreactor through the Use of a Novel Holographic Correlation Velocimetry Flow Measurement Technique. *PLoS ONE* **2013**, *8*, e65714. [CrossRef] [PubMed]
30. Markus, R.; Willert, C.E.; Scarano, F. *Particle Image Velocimetry: A Practical Guide*, 3rd ed.; Springer: Berlin/Heidelberg, Germany, 2018.
31. Keane, R.D.; Adrian, R.J. Theory of Cross-Correlation Analysis of PIV Images. *Appl. Sci. Res.* **1992**, *49*, 191–215. [CrossRef]
32. Dong, R.R.; Katz, J.; Huang, T.T. On the Structure of Bow Waves on a Ship Model. *J. Fluid Mech.* **1997**, *346*, 77–115. [CrossRef]
33. Tukker, J.; Blok, J.J.; Kuiper, G.; Huijsmans, R.H.M. Wake Flow Measurements in Towing Tanks with PIV. In Proceedings of the Ninth International Symposium on Flow Visualization, Edinburgh, UK, 22–25 August 2000; pp. 1–6.
34. Baghaie, A. Robust Principal Component Analysis for Background Estimation of Particle Image Velocimetry Data. In Proceedings of the 2019 IEEE Long Island Systems, Applications and Technology Conference (LISAT), New York, NY, USA, 3 May 2019; pp. 1–6.
35. Jux, C.; Sciacchitano, A.; Schneiders, J.; Scarano, F. Robotic Volumetric PIV of a Full-Scale Cyclist. Exp. *Fluids* **2018**, *59*, 74. [CrossRef]
36. Lee, S.K.; Giacobello, M.; Manovski, P.; Kumar, C. Optimising Camera Arrangement for Stereoscopic Particle Image Velocimetry. In Proceedings of the 19th Australasian Fluid Mechanics Conference, Melbourne, Australia, 8 December 2104.
37. Egeberg, T.F.; Yoon, H.; Stern, F.; Pettersen, B.; Bhushan, S. Vortex Shedding from a Ship Hull by Means of Tomographic PIV. In Proceedings of the International Conference on Offshore Mechanics and Arctic Engineering, San Francisco, CA, USA, 8 June 2014.

38. Wang, B.; Liao, Q.; Xiao, J.; Bootsma, H.A. A Free-Floating PIV System: Measurements of Small-Scale Turbulence under the Wind Wave Surface. *J. Atmos. Ocean. Technol.* **2013**, *30*, 1494–1510. [CrossRef]
39. Galani, K.A.; Dimas, A.A. Experimental Study of the Influence of Wave Breaking Over a Sloping Beach on the Flow Upstream of the Surf Zone. In Proceedings of the 27th International Ocean and Polar Engineering Conference, San Francisco, CA, USA, 25–30 June 2017.
40. Pope, S.B. *Turbulent Flows*; Cambridge University Press: Cambridge, UK, 2000; ISBN 9780521598866.
41. Seo, J.; Han, B.; Rhee, S.H. Towed Underwater SPIV Measurement of Flow Fields Around a Surface-Piercing Cylinder with Free Surface Effects. In Proceedings of the Fluids Engineering Division Summer Meeting, Seoul, Korea, 26–31 July 2015.
42. Muthanna, C.; Visscher, J.; Pettersen, B. Investigating Fluid Flow Phenomena behind Intersecting and Tapered Cylinders Using Submerged Stereoscopic PIV. In Proceedings of the 14th International Symposium on Applications of Laser Techniques to Fluid Mechanics, Lisboa, Portugal, 7–10 July 2008.
43. Yoon, H.; Longo, J.; Toda, Y.; Stern, F. Benchmark CFD Validation Data for Surface Combatant 5415 in PMM Maneuvers—Part II: Phase-Averaged Stereoscopic PIV Flow Field Measurements. *Ocean Eng.* **2015**, *109*, 735–750. [CrossRef]
44. Han, B.W.; Seo, J.; Lee, S.J.; Seol, D.M.; Rhee, S.H. Uncertainty Assessment for a Towed Underwater Stereo PIV System by Uniform Flow Measurement. *Int. J. Nav. Archit. Ocean Eng.* **2018**, *10*, 596–608. [CrossRef]
45. ITTC. *Uncertainty Analysis Particle Imaging Velocimetry*; ITTC: Zürich, Switzerland, 2008.
46. Go, S.C.; Seo, J.; Park, J.; Rhee, S.H. Towed Underwater PIV Measurement of Propeller Wake in Self-Propelled Condition. *Exp. Fluids* **2019**, *60*, 184. [CrossRef]
47. Seo, J.; Lee, S.J.; Choi, W.S.; Park, S.T.; Rhee, S.H. Experimental Study on Kinetic Energy Conversion of Horizontal Axis Tidal Stream Turbine. Renew. *Energy* **2016**, *97*, 784–797. [CrossRef]
48. Jacobi, G.; Thill, C.; Huijsmans, R. The Application of Particle Image Velocimetry for the Analysis of High-Speed Craft Hydrodynamics. In Proceedings of the Conference on Hydrodynamics-ICHD, Egmond aan Zee, The Netherlands, 18–23 September 2016.
49. Ashworth Briggs, A.; Fleming, A.; Duffy, J.; Binns, J.R. Tracking the Vortex Core from a Surface-Piercing Flat Plate by Particle Image Velocimetry and Numerical Simulation. *Proc. Inst. Mech. Eng. Part M J. Eng. Marit. Environ.* **2019**, *233*, 793–808. [CrossRef]
50. Yagmur, S.; Dogan, S.; Aksoy, M.H.; Goktepeli, I.; Ozgoren, M. Comparison of Flow Characteristics around an Equilateral Triangular Cylinder via PIV and Large Eddy Simulation Methods. *Flow Meas. Instrum.* **2017**, *55*, 23–36. [CrossRef]
51. EU Funded Project Hiprwind. Available online: http://hiprwind.eu/ (accessed on 1 January 2020).
52. Olsen, M.G.; Adrian, R.J. Brownian Motion and Correlation in Particle Image Velocimetry. *Opt. Laser Technol.* **2000**, *32*, 621–627. [CrossRef]
53. Catipovic, M.A.; Tyler, P.M.; Trapani, J.G.; Carter, A.R. Improving the Quantification of Brownian Motion. *Am. J. Phys.* **2013**, *81*, 485–491. [CrossRef]
54. Al-Muhammad, J.; Tomas, S.; Ait-Mouheb, N.; Amielh, M.; Anselmet, F. Micro-PIV Characterization of the Flow in a Milli-Labyrinth-Channel Used in Drip Irrigation. *Exp. Fluids* **2018**, *59*, 181. [CrossRef]
55. Desmond, C.; Murphy, J.; Blonk, L.; Haans, W. Description of an 8 MW Reference Wind Turbine. *J. Phys. Conf. Ser.* **2016**, *753*, 092013. [CrossRef]
56. Schröder, A.; Willert, C.; Schanz, D.; Geisler, R.; Jahn, T.; Gallas, Q.; Leclaire, B. The Flow around a Surface Mounted Cube: A Characterization by Time-Resolved PIV, 3D Shake-The-Box and LBM Simulation. *Exp. Fluids* **2020**, *61*, 189. [CrossRef]
57. Desmond, C.; Buret, B.; Shanley, M.; Murphy, J.; Pakrashi, V. The Assessment of Water Surface Elevation Uncertainty in a Hydraulics Laboratory. In Proceedings of the 13th International Conference on Applications of Statistics and Probability in Civil Engineering (ICASP13), Seoul, Korea, 26–30 May 2019.
58. Chong, K.L.; Shi, J.Q.; Ding, G.Y.; Ding, S.S.; Lu, H.Y.; Zhong, J.Q.; Xia, K.Q. Vortices as Brownian Particles in Turbulent Flows. *Sci. Adv.* **2020**, *6*, eaaz1110. [CrossRef]
59. Smith, C. *Guidance on the Safe Use of Lasers*; Trinity College Dublin: Dublin, Ireland, 2015.
60. Sciacchitano, A. Uncertainty Quantification in Particle Image Velocimetry. *Meas. Sci. Technol.* **2019**, *30*, 092001. [CrossRef]
61. Adrian, R.J.; Westerweel, J. *Particle Image Velocimetry*; Cambridge Aerospace Series; Cambridge University Press: Cambridge, UK, 2011; ISBN 9780521440080.
62. Grizzi, S.; Pereira, F.; Di Felice, F. A Simplified, Flow-Based Calibration Method for Stereoscopic PIV. *Exp. Fluids* **2010**, *48*, 473–486. [CrossRef]
63. Prasad, A.K. Particle Image Velocimetry. *Curr. Sci.* **2000**, *79*, 51–60.
64. Wieneke, B. PIV Uncertainty Quantification and Beyond. Ph.D. Thesis, Delft University of Technology, Delft, The Netherlands, 2017.
65. Jurgens, A. Experimental Investigation into the Flow around a Manoeuvring LNG carrier on Shallow Water. In Proceedings of the NAV International Conference on Ship and Shipping Research, Cetena, Genova, 21–23 June 2006.
66. Garcia, D. A Fast All-in-One Method for Automated Post-Processing of PIV Data. *Exp. Fluids* **2011**, *50*, 1247–1259. [CrossRef]
67. Liu, Z.; Jia, L.; Zheng, Y.; Zhang, Q. Flow-Adaptive Data Validation Scheme in PIV. *Chem. Eng. Sci.* **2008**, *63*, 1–11. [CrossRef]
68. Pun, C.-S.; Susanto, A.; Dabiri, D. Mode-Ratio Bootstrapping Method for PIV Outlier Correction. *Meas. Sci. Technol.* **2007**, *18*, 3511. [CrossRef]
69. Timmins, B.; Wilson, B.; Smith, B.; Vlachos, P. A Method for Automatic Estimation of Instantaneous Local Uncertainty in Particle Image Velocimetry Measurements. *Exp. Fluids* **2012**, *53*, 1133–1147. [CrossRef]

70. Charonko, J.J.; Vlachos, P.P. Estimation of Uncertainty Bounds for Individual Particle Image Velocimetry Measurements from Cross-Correlation Peak Ratio. *Meas. Sci. Technol.* **2013**, *24*, 65301. [CrossRef]
71. Scharnowski, S.; Kähler, C. On the Loss-of-correlation Due to PIV Image Noise. *Exp. Fluids* **2016**, *57*, 119. [CrossRef]
72. Kähler, C.; Cierpka, C.; Scharnowski, S. On the Uncertainty of Digital PIV and PTV near Walls. *Exp. Fluids* **2012**, *52*, 1641–1656. [CrossRef]
73. Bhattacharya, S.; Charonko, J.; Vlachos, P. Particle Image Velocimetry (PIV) Uncertainty Quantification Using Moment of Correlation (MC) Plane. *Meas. Sci. Technol.* **2018**, *29*, 115301. [CrossRef]
74. Neal, D.; Sciacchitano, A.; Smith, B.; Scarano, F. Collaborative Framework for PIV Uncertainty Quantification: The Experimental Database. *Meas. Sci. Technol.* **2015**, *26*, 074003. [CrossRef]
75. Song, K.; Guo, C.; Wang, C.; Gong, J.; Li, P. Investigation of the Influence of an Interceptor on the Inlet Velocity Distribution of a Waterjet-Propelled Ship Using SPIV Technology and RANS Simulation. *Ships Offshore Struct.* **2020**, *15*, 138–152. [CrossRef]
76. Murfet, T.; Abdussamie, N. Loads and Response of a Tension Leg Platform Wind Turbine with Non-Rotating Blades: An Experimental Study. *J. Mar. Sci. Eng.* **2019**, *7*, 54. [CrossRef]
77. Det Norske Veritas (DNV). *DNV-RP-C205 Environmental Conditions and Environmental Loads*; Det Norske Veritas (DNV): Bærum, Norway, 2010.
78. Robertson, A.; Jonkman, J.; Masciola, M.; Song, H.; Goupee, A.; Coulling, A.; Luan, C. *Definition of the Semisubmersible Floating System for Phase II of OC4*; National Renewable Energy Lab. (NREL): Golden, CO, USA, 2014.
79. Zhou, Y.; Xiao, Q.; Liu, Y.; Incecik, A.; Peyrard, C.; Li, S.; Pan, G. Numerical Modelling of Dynamic Responses of a Floating Offshore Wind Turbine Subject to Focused Waves. *Energies* **2019**, *12*, 3842. [CrossRef]
80. Deng, R.; Wang, S.; Luo, W.; Wu, T. Experimental Study on the Influence of Bulbous Bow Form on the Velocity Field around the Bow of a Trimaran Using Towed Underwater 2D-3C SPIV. *J. Mar. Sci. Eng.* **2021**, *9*, 905. [CrossRef]
81. Ruesink, W.G. *Introduction to Sampling Theory BT—Sampling Methods in Soybean Entomology*; Kogan, M., Herzog, D.C., Eds.; Springer: New York, NY, USA, 1980; pp. 61–78, ISBN 978-1-4612-9998-1.
82. Xu, Q.; Li, Y.; Yu, Y.-H.; Ding, B.; Jiang, Z.; Lin, Z.; Cazzolato, B. Experimental and Numerical Investigations of a Two-Body Floating-Point Absorber Wave Energy Converter in Regular Waves. *J. Fluids Struct.* **2019**, *91*, 102613. [CrossRef]
83. Fuat, K. Multibody Interactions of Floating Bodies with Time-Domain Predictions. J. Waterw. Port Coast. *Ocean Eng.* **2020**, *146*, 4020031. [CrossRef]
84. Robertson, A.N.; Wendt, F.; Jonkman, J.M.; Popko, W.; Dagher, H.; Gueydon, S.; Qvist, J.; Vittori, F.; Azcona, J.; Uzunoglu, E.; et al. OC5 Project Phase II: Validation of Global Loads of the DeepCwind Floating Semisubmersible Wind Turbine. *Energy Procedia* **2017**, *137*, 38–57. [CrossRef]
85. Robertson, A. *Integrated Systems Design and Analysis Offshore Wind Project ID #T10*; National Renewable Energy Laboratory (NREL): Golden, CO, USA, 2019.
86. Carlson, D.W.; Modarres-Sadeghi, Y. Vortex-Induced Vibration of Spar Platforms for Floating Offshore Wind Turbines. *Wind Energy* **2018**, *21*, 1169–1176. [CrossRef]
87. Pan, J.; Ishihara, T. Nonlinear Wave Effects on Dynamic Responses of a Semisubmersible Floating Offshore Wind Turbine in the Intermediate Water. *J. Phys. Conf. Ser.* **2018**, *1037*, 022037. [CrossRef]
88. Xu, K.; Shao, Y.; Gao, Z.; Moan, T. A Study on Fully Nonlinear Wave Load Effects on Floating Wind Turbine. *J. Fluids Struct.* **2019**, *88*, 216–240. [CrossRef]
89. Hedges, T.S.; Tickell, R.G.; Akrigg, J. Interaction of Short-Crested Random Waves and Large-Scale Currents. *Coast. Eng.* **1993**, *19*, 207–221. [CrossRef]
90. Wang, P.; Zhao, M.; Du, X. Short-Crested Wave-Current Forces on Composite Bucket Foundation for an Offshore Wind Turbine. *Math. Probl. Eng.* **2019**, *2019*, 5932742. [CrossRef]
91. Wei, Z.; Dalrymple, R.A. SPH Modeling of Short-Crested Waves. *arXiv* **2017**, arXiv:1705.08547.
92. Vasarmidis, P.; Stratigaki, V.; Troch, P. Accurate and Fast Generation of Irregular Short Crested Waves by Using Periodic Boundaries in a Mild-Slope Wave Model. *Energies* **2019**, *12*, 785. [CrossRef]
93. Cheng Yee, N.; Tuhaijan, S.N.A.; Fattah, M.Z.A.; John Kurian, V.; Mustaffa, Z. Experimental Investigation of Directional Hydrodynamic Coefficients and the Effects on Wave Force Due to Spreading Angles. *Ain Shams Eng. J.* **2020**, *11*, 1021–1034. [CrossRef]
94. Martinez-Luengo, M.; Causon, P.; Gill, A.B.; Kolios, A.J. The Effect of Marine Growth Dynamics in Offshore Wind Turbine Support Structures. In Proceedings of the 6th International Conference on Marine Structures, Lisbon, Portugal, 8–10 May 2017; pp. 889–898.
95. *DNV-OS-J101: Design of Offshore Wind Turbine Structures*; DNV: Bærum, Norway, 2014.
96. *API 2A-WSD: Planning, Designing, and Constructing Fixed Offshore Platforms—Working Stress Design*; American Petroleum Institute (API): Washington, DC, USA, 2014.
97. Pham, H.; Veritas, B.; Arnal, V.; Nantes, E.C. De Effect of Marine Growth on Floating Wind Turbines Mooring Lines Responses Abstract. In Proceedings of the Congrès Français de MécaniqueAt, Lille, France, 1–8 September 2017.
98. Chuang, T.C.; Yang, W.H.; Yang, R.Y. Experimental and Numerical Study of a Barge-Type FOWT Platform under Wind and Wave Load. *Ocean Eng.* **2021**, *230*, 109015. [CrossRef]

99. Ticona Rollano, F.; Brown, A.; Ellenson, A.; Özkan-Haller, H.T.; Thomson, J.; Haller, M.C. Breaking Waves in Deep Water: Measurements and Modeling of Energy Dissipation. *Ocean Dyn.* **2019**, *69*, 1165–1179. [CrossRef]
100. Liu, S.; Ong, M.; Obhrai, C. Numerical Simulations of Breaking Waves and Steep Waves Past a Vertical Cylinder at Different Keulegan–Carpenter Numbers. *J. Offshore Mech. Arct. Eng.* **2019**, *141*, 041806. [CrossRef]
101. Ye, K.; Ji, J. Current, Wave, Wind and Interaction Induced Dynamic Response of a 5 MW Spar-Type Offshore Direct-Drive Wind Turbine. *Eng. Struct.* **2019**, *178*, 395–409. [CrossRef]
102. Chen, L.; Basu, B. Wave-Current Interaction Effects on Structural Responses of Floating Offshore Wind Turbines. *Wind Energy* **2019**, *22*, 327–339. [CrossRef]
103. Clement, C.; Kosleck, S.; Lie, T. Investigation of Viscous Damping Effect on the Coupled Dynamic Response of a Hybrid Floating Platform Concept for Offshore Wind Turbines. *Ocean Eng.* **2021**, *225*, 108836. [CrossRef]
104. Wang, L.; Robertson, A.; Jonkman, J.; Yu, Y.-H.; Koop, A.; Borràs Nadal, A.; Li, H.; Shi, W.; Pinguet, R.; Zhou, Y.; et al. Investigation of Nonlinear Difference-Frequency Wave Excitation on a Semisubmersible Offshore-Wind Platform With Bichromatic-Wave CFD Simulations. In Proceedings of the International Conference on Offshore Mechanics and Arctic Engineering, Hamburg, Germany, 5–10 June 2021.
105. Tiwari, N.; Tasaka, Y.; Murai, Y. PIV-Based Estimation of Viscosity and Pressure Fields for a Steady Pseudoplastic Flow. *Flow Meas. Instrum.* **2021**, *77*, 101852. [CrossRef]
106. Lemmer, F.; Yu, W.; Luhmann, B.; Schlipf, D.; Cheng, P.W. Multibody Modeling for Concept-Level Floating Offshore Wind Turbine Design. *Multibody Syst. Dyn.* **2020**, *49*, 203–336. [CrossRef]
107. Ma, Z.; Wang, S.; Wang, Y.; Ren, N.; Zhai, G. Experimental and Numerical Study on the Multi-Body Coupling Dynamic Response of a Novel Serbuoys-TLP Wind Turbine. *Ocean Eng.* **2019**, *192*, 106570. [CrossRef]
108. Al-Solihat, M.K.; Nahon, M. Flexible Multibody Dynamic Modeling of a Floating Wind Turbine. *Int. J. Mech. Sci.* **2018**, *142*, 518–529. [CrossRef]
109. Wang, L.; Robertson, A.; Jonkman, J.; Yu, Y.H. Uncertainty Assessment of CFD Investigation of the Nonlinear Difference-Frequency Wave Loads on a Semisubmersible FOWT Platform. *Sustainability* **2021**, *13*, 64. [CrossRef]